Partial Cavity Instabilities and Re-Entrant Jet

J.P. Franc

Laboratoire des Ecoulements Géophysiques et Industriels, BP 53, 38041 GRENOBLE Cedex 9, France

Abstract

The purpose of this talk is to give an overview of different instabilities which can affect partial cavitation. We shall focus on the case of a unique partial cavity attached to an isolated hydrofoil or to the throat of a Venturi. Another paper presented by Tsujimoto (2001) in this conference is dedicated to cavitation instabilities in turbomachinery, where several cavities are simultaneously present and can interact. In this paper, we have deliberately chosen to emphasize some particular aspects of partial cavity instabilities, especially the re-entrant jet instability and the associated cloud cavitation. Some discussions reflect our personal point of view on a subject still in progress.

1. Introduction

We are mainly concerned here with partial cavities, i.e. cavities which detach from the vicinity of the leading edge of a hydrofoil and close on the wall. Partial cavitation is opposed to supercavitation, which refers to long cavities whose length is greater than the chord length of the hydrofoil and therefore which close in the fluid bulk.

Partial cavities are unsteady in nature. Unsteadiness has long been an obstacle to the experimental and theoretical analysis of partial cavitation. From a modelling viewpoint for instance, it has been necessary to develop specific models to force partial cavities to close within the framework of *steady* computations. Yamaguchi and Kato (1983), in their non-linear steady theory of cavity flow, solve the Rayleigh-Plesset equation for a single spherical bubble to estimate a "mean" cavity shape in the closure region. Lemonnier and Rowe (1988) introduce a special steady model of the cavity-wake to get round the unsteady feature of the cavity closure. Such tricks are no more necessary because of the progress in computers which makes possible unsteady computations. Unsteadiness is a necessary ingredient for a partial cavity to close naturally.

The inherent unsteady nature of partial cavities leads to more or less important fluctuations of their length. Such fluctuations are generally referred to as partial cavitation instabilities. The term instability is used to qualify such situations in which no steady cavity actually exists.

The observation of partial cavities under various conditions leads to the conclusion that the characteristic size of the region in which unsteady effects are significant is variable. Figure 1b presents the case of a highly unsteady partial cavity for which unsteadiness affects almost the whole cavity, up to its detachment. The situation is very different in the case of Figure 1a for which unsteadiness is confined in a relatively small region, so that the cavity can be considered as stable, at least from a large scale viewpoint. Therefore, it seems important to associate, to the cavity closure, a length scale which characterizes the extent of unsteadiness. It can be considered as the difference between the minimum and maximum cavity lengths. It gives the length scale of the largest vapor structures which are shed (cf. Figure 7).

We propose to distinguish two main classes of instabilities, *intrinsic* instabilities and *system* instabilities, according to the origin of the unsteadiness. In the case of a system instability, the unsteady behaviour comes from the interaction between the cavity and the rest of the system. By system, we mean the environment of the cavity. In the case of a cavitation tunnel for example, the inlet or outlet lines as well as the tanks are parts of the hydraulic system which may influence the development of the instabilities. In the case of a turbomachinery, if we consider the cavity which develops on a given blade, it may interact with the other cavities attached to the other blades. The case of alternate blade cavitation or rotating cavitation observed in inducers (Tsujimoto 2001) is a typical example of system instability involving multiple cavities[1]. The origin of this kind of instability lies in the interaction between the various cavities. Roughly speaking, if, for some reason, the length of a given cavity is changed, the streamlines

---

[1] Alternate blade cavitation is generally considered as a cavitation instability although each cavity has a constant length. It is the difference of cavity length from one blade to another which justifies the term instability.

are changed and the angle of attack of the neighbouring blades is also changed, leading to a modification in the length of the other cavities. It is not easy to guess the final configuration, which is often unsteady, from so simple arguments. But computational techniques are now available to predict such instabilities (Tsujimoto 2001). It follows that, for a system instability, the dynamic behaviour of the cavity depends drastically upon its environment.

On the contrary, an intrinsic instability originates in the cavity itself. Its features, as its frequency content, are independent of the circuit. The fact that the dynamic behaviour of a cavity is independent of the characteristics of the environment is the best proof of the intrinsic nature of the instability. For instance, it is well known that the re-entrant jet instability gives birth to oscillations of the cavity length. Many experiments, conducted in various testing facilities around the world, with very different hydraulic impedances, lead to oscillation frequencies which proved to be almost the same in terms of Strouhal numbers. Hence, the re-entrant jet instability and associated cloud cavitation is clearly of intrinsic type.
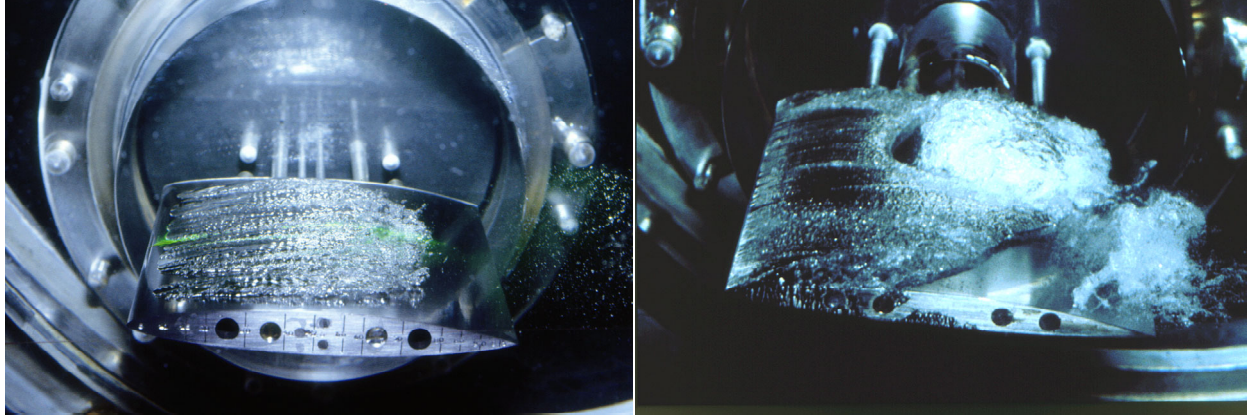

Figure 1: Visualizations of partial cavities on a two-dimensional hydrofoil in a cavitation tunnel.

2. System instabilities

Cavitation surge is a typical example of system instability. To illustrate it, let us consider a cavitating hydrofoil in a duct of area A (Figure 2). A simplified one-dimensional model is used to analyse this configuration (Watanabe *et al.*, 1998). For simplicity, the downstream length is supposed infinite, so that the mass flowrate m in the downstream line remains constant because of an infinite inertia. In steady conditions, the cavity volume ϑ is constant and the mass flowrate m as well as the pressure p in any section are constant if head losses are neglected. Under unsteady conditions, we denote m'(t) the fluctuation of mass flowrate in the upstream line and p'(t) the pressure fluctuation at the location of the hydrofoil. The inlet pressure is supposed constant. The momentum balance in the upstream duct can be written:

$$-\frac{L}{A}\frac{dm'}{dt} = p' \qquad (1)$$

The mass balance simply expresses that the variations in cavity volume are balanced by the fluctuations in the incoming flowrate:

$$m' = -\rho\frac{d\vartheta}{dt} \qquad (2)$$

The variations in cavity volume are linearly related to the variations in pressure by introducing the classical cavitation compliance K:

$$\rho\frac{d\vartheta}{dt} = -K\frac{dp'}{dt} \qquad (3)$$

It is important to notice that the cavitation compliance results from purely quasi-static considerations and do not involve any dynamic feature of the cavity.

By combining the three previous equations, we get the following equation for the pressure fluctuation:

$$\frac{d^2p'}{dt^2} + \frac{A}{LK}p' = 0 \qquad (4)$$

2

The type of solution depends upon the sign of the cavitation compliance K. If K is positive, all the variables exhibit periodic oscillations at the frequency:

$$\omega = \sqrt{\frac{A}{LK}} \tag{5}$$

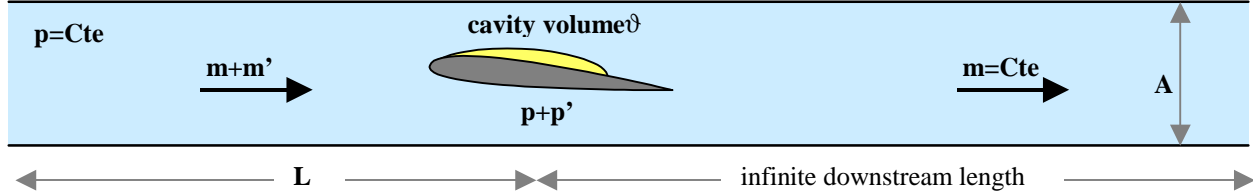which is the natural frequency of the system made of the cavity and the inlet line.

Figure 2: The case of an isolated cavitating foil in a duct. For simplicity, the downstream length is supposed infinite

This regime is typical of surge cavitation. The physical reason for oscillations is easy to understand. If it is supposed that the pressure at the location of the hydrofoil decreases, the cavity volume increases because of a positive value of the cavitation compliance. By continuity, the incoming flowrate decreases and the inertia of the upstream column makes the pressure at the location of the hydrofoil increase. Hence, the situation is stable and auto-oscillations develop.

From Equation 5, it appears that the frequency of the pulsations results from a coupling between the cavity, characterized by its compliance, and the inlet line, characterized by its length L and area A. This behaviour is typical of a system instability.

In the case of a negative cavitation compliance, the solution is no more periodic but increases exponentially. The behaviour is unstable. A negative cavitation compliance corresponds to a decrease in cavity volume with a decrease in pressure, which is not the usual trend. Figure 3 presents a typical variation of the cavity length with the cavitation parameter. The qualitative shape of this curve is the same, whatever may be the hydrofoil. From the experimental results, it is clear that the cavitation compliance is always positive, in the partial cavitation domain, as well as in the supercavitation one. Also indicated in Figure 3 are the predicted curves from classical linearized theory applied to a flat plate (Brennen 1995). It appears that the cavitation compliance is negative for ratios of the cavity length to the chord length between ¾ and 1. This argument is sometimes used to explain the instability that some experimenters have observed between partial and supercavitation, when the cavity length exhibits oscillations around $L/c \approx 1$ (see e.g. Wade & Acosta 1966). This region of negative cavitation compliance results from a mathematical artefact due to the change of model between partial and supercavitation. In our opinion, it has no physical origin, as the experimental results tend to prove and therefore, it is probably not the reason for the instability between partial and supercavitation, which is more likely of surge type.

Another interesting feature of the curves $L(\sigma)$ with respect to cavitation instabilities is the large variation of slope, i.e. of cavitation compliance. For small enough cavitation parameters, the slope and the cavitation compliance are large, contrary to the case of large cavitation parameters. Hence, small fluctuations in cavitation parameter will generate large fluctuations in cavity length as also shown by Equation 3. In other words, long cavities exhibit an extreme sensitivity to external fluctuations that small cavities do not. This phenomenon directly influences the amplitude of the cavity oscillations.

This difference of behaviour between short and long cavities can be related to differences in adverse pressure gradient in the closure region. As schematically shown on Figure 4, it is expected that the longer the cavity on a hydrofoil, the smaller the adverse pressure gradient at closure. The magnitude of the adverse pressure gradient can be considered as a basic physical parameter which controls the fluctuations in cavity length. It behaves like an obstacle to the development of the cavity. If the pressure gradient at closure is high, the cavity experiences a strong resistance to grow. On the contrary, if the pressure distribution is relatively flat, the cavity can grow more easily.

Above, we examined the basic case of cavitation surge for an isolated hydrofoil in a duct. The principle of the analysis remains applicable to more complicated cases. As an example, we mention the work of Duttweiler (2001) who explored a surge instability on a cavitating propeller tested in a water tunnel. The procedure he developed illustrates the main steps to follow, in order to analyse a cavitation surge instability. The cavitation dynamics and the

facility dynamics are considered as part of a coupled system. Each of them has to be characterized in order to predict the whole system dynamics. The main steps of the prediction are the following.

1. The quasi-steady response of the cavitation volume to changes in inlet conditions is characterized in terms of a cavitation compliance K and a mass flow gain factor M. The cavitation compliance describes the variation in cavity volume with the pressure (cf. Equation 3), whereas the mass flow gain factor describes the variation in cavity volume with the angle of attack. The mass flow gain factor is needed for the modelling of cavitation instabilities in turbomachinery, because a change in inlet flow rate results in a change in angle of attack, as it can be seen from the consideration of the velocity triangle.

2. The second step consists in modelling the dynamics of the facility by dividing it into elementary components (pipes, tanks…) of specified resistance, capacitance and inertance.

3. Finally, the facility dynamics and the cavitation dynamics have to be combined in order to identify potentially unstable behaviours.

By applying the previous procedure to the case of a propeller in a cavitation tunnel, Duttweiler (2001) succeeded in predicting the characteristic frequency of the observed instability. This procedure can be followed for the analysis of any partial cavity instability of surge type.
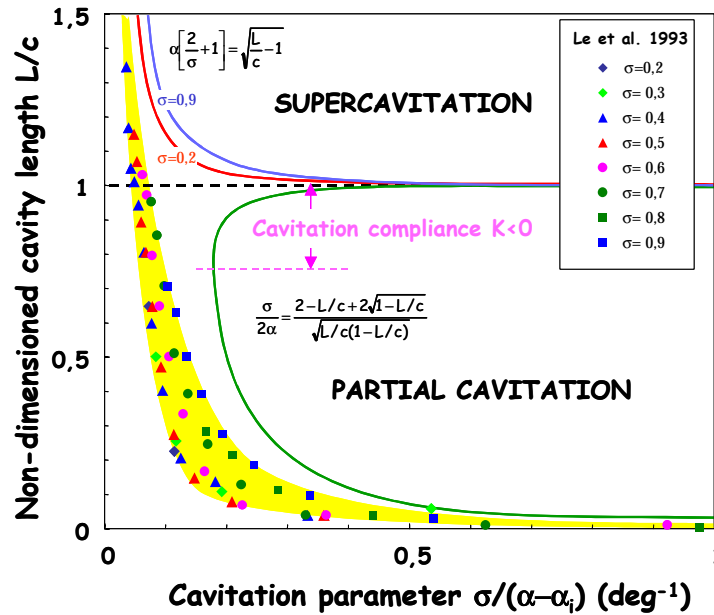

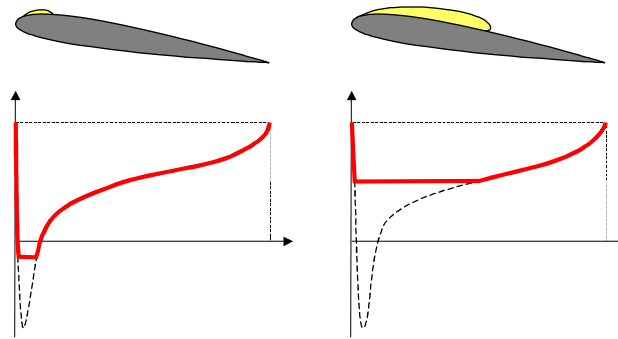*Figure 3: Typical variation of the cavity length L with the cavitation parameter*

Figure 4: Cavity length and pressure gradient (qualitative sketch).

4

3. Re-entrant jet and cloud cavitation instability

Re-entrant jet

The re-entrant jet instability is the most typical example of intrinsic instability. It has been described by many researchers. Thirty years ago, Knapp, Daily and Hammitt have given a rather precise description of the flow at the rear end of a cavity. The cavity closure is the region where the external flow re-attaches to the wall. The flow which originally moves along the cavity has locally the structure of a jet impinging obliquely upon the wall. The falling stream divides into two parts flowing parallel to the wall. One is the re-entrant jet which moves upstream towards the cavity detachment. The other one makes the flow re-attach to the wall.

In the framework of steady potential flow analysis, it is possible to have a picture of the rear part of an attached cavity (Figure 5) and in particular to obtain an estimate of the thickness of the re-entrant jet (Figure 6). In the simple case of a cavity behind a step in a semi-infinite medium, the classical non-linear theory (Michel, 1978) gives the thickness of the re-entrant jet λ as a function of the cavitation parameter σ:

$$\lambda = \frac{1}{2}\left[1 - \frac{1}{\sqrt{1+\sigma}}\right] \tag{6}$$

In this equation, the step height is chosen as unity. The smaller the cavitation parameter, the longer the cavity, the smaller the impingement angle and the smaller the re-entrant jet thickness.
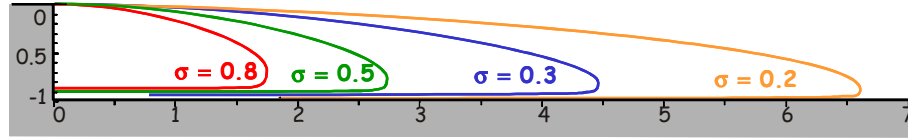

Figure 5: Non-linear steady potential flow computation of the shape of the cavity behind a step in a semi-infinite medium. The shape of the cavity is given by the following equations $x(r) = \frac{\lambda}{\pi}\left[\frac{1 - 2\lambda + 2\lambda^2}{\lambda^2}r + \ln(1-r)\right]$ *and*
$y(r) = -(1-\lambda)\left[1 - \frac{1}{\pi}\cos^{-1}(2r-1) - \frac{2}{\pi}\sqrt{r(1-r)}\right]$ *where r is a mathematical parameter varying between 0 at detachment and 1 at the infinity end of the re-entrant jet. The cavity length is given by*

$$L = \frac{\lambda}{\pi}\left[\frac{(1-\lambda)^2}{\lambda^2} + \ln\frac{\lambda^2}{1 - 2\lambda + 2\lambda^2}\right]$$
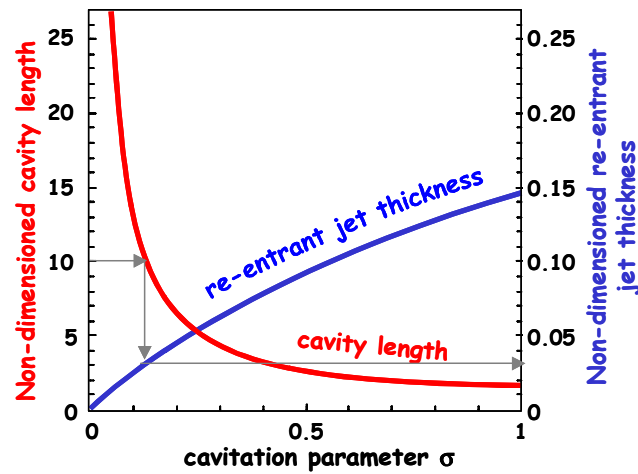

Figure 6: Variations of the re-entrant jet thickness and of the cavity length for a 2D cavity behind a step in a semi-infinite medium. Non linear steady potential flow computation.

The previous case of a step in a semi-infinite medium corresponds to a negligible adverse pressure gradient. In many practical cases, in particular for a hydrofoil or a Venturi, a mean pressure gradient is imposed by the flow. In the case of a Venturi e.g., the mean pressure increases because of the divergence. The pressure gradient affects the development of the re-entrant jet: an adverse pressure gradient will reinforce it, whereas a favourable pressure gradient, if any, would reduce its thickness. To precisely quantify this effect, it is necessary to carry out a complete calculation of the cavity flow and examples will be given later. However, an order of magnitude can easily be obtained from a dimensional analysis. A simplified model (Callenaere *et al.*, 2001) leads to the following estimate of the re-entrant jet thickness in the case of a pressure gradient:

$$\lambda \approx \lambda_0 + \frac{1}{4}\frac{dC_p}{d(x/L)} \tag{7}$$

In this equation, the cavity thickness is still used as the unit length scale. The quantity λ_0 holds for the thickness of the re-entrant jet without any pressure gradient. It can be estimated from Equation 6. The second term gives an account of the influence of the pressure gradient on the re-entrant jet thickness. The relevant length scale for the calculation of the pressure coefficient gradient is the cavity length L. Quantitative estimates will be given later. Nevertheless, it is clear from Equation 7 that an adverse pressure gradient is favourable to the re-entrant jet and increases its thickness. This effect of the pressure gradient on the re-entrant jet is essential in the analysis of the cloud cavitation instability as it is well-known that the re-entrant jet is the source of the cloud cavitation instability.

Unsteady behaviour

The former analysis lies upon a steady approach. However, the re-entrant jet cannot exist continually, otherwise the cavity would be filled out with liquid. Hence, we are lead to suppose that a succession exists between periods of development of the re-entrant jet, which tend to fill the cavity, and periods of emptying and entrainment of the two-phase mixture. This phenomenon is essentially controlled by inertia. A simple dimensional analysis leads to the conclusion that the oscillation frequency f is of the order of L/V_∞. Actually, the Strouhal number $S=f L /V_\infty$ of this instability, based on the maximum cavity length L, was found to range between about 0.25 and 0.4 by many experimenters (see e.g. Kawanami *et al.* 1998 for a comparison of results of various origins).

The Strouhal number can be interpreted as the ratio of the time required by the re-entrant jet to reach the cavity leading edge L/V_∞ to the period of the oscillation 1/f. We shall see later that the velocity of the re-entrant jet is of the order of the flow velocity V_∞, which justifies the estimate L/V_∞ for the time required by the re-entrant jet to reach the cavity leading edge. The use of the cavity length as the characteristic length scale in the Strouhal number is relevant if the re-entrant jet actually reaches the leading edge of the cavity. In some cases, it cuts the cavity interface far before the cavity leading edge. If so, the size of the shedded vapour structures which characterizes the extent of unsteadiness at closure is much smaller than the cavity length (Figure 7). A few experiments (Belahadji *et al.* 1997) tend to prove that the Strouhal number still remains within the former range, provided it is based upon the characteristic length L of the shedded structures, which does not necessarily correspond to the cavity length. If this conjecture is confirmed, it would mean that a cavity which sheds small vapour structures should exhibit a relatively high oscillation frequency.
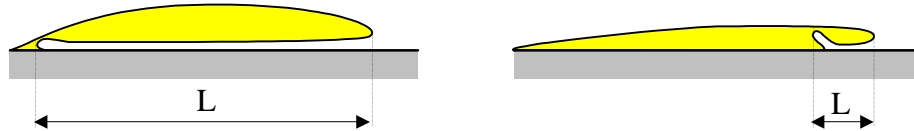

Figure 7: Schematic interpretation of the characteristic length scale at closure

Figure 8 presents a visualization of the cycle of the cloud cavitation instability in the case of a cavity behind a diverging step. The various phases including the progression of the re-entrant jet, the shedding of a vapour structure and the growth of the leading edge cavity can be identified. The re-entrant jet is initiated around image 0.42 T. It moves upstream and reaches the leading edge around time 0.73 T. Then a cavitation cloud is formed and entrained by the main flow. The leading edge cavity grows progressively between images 0.84 T and 0.31 T.
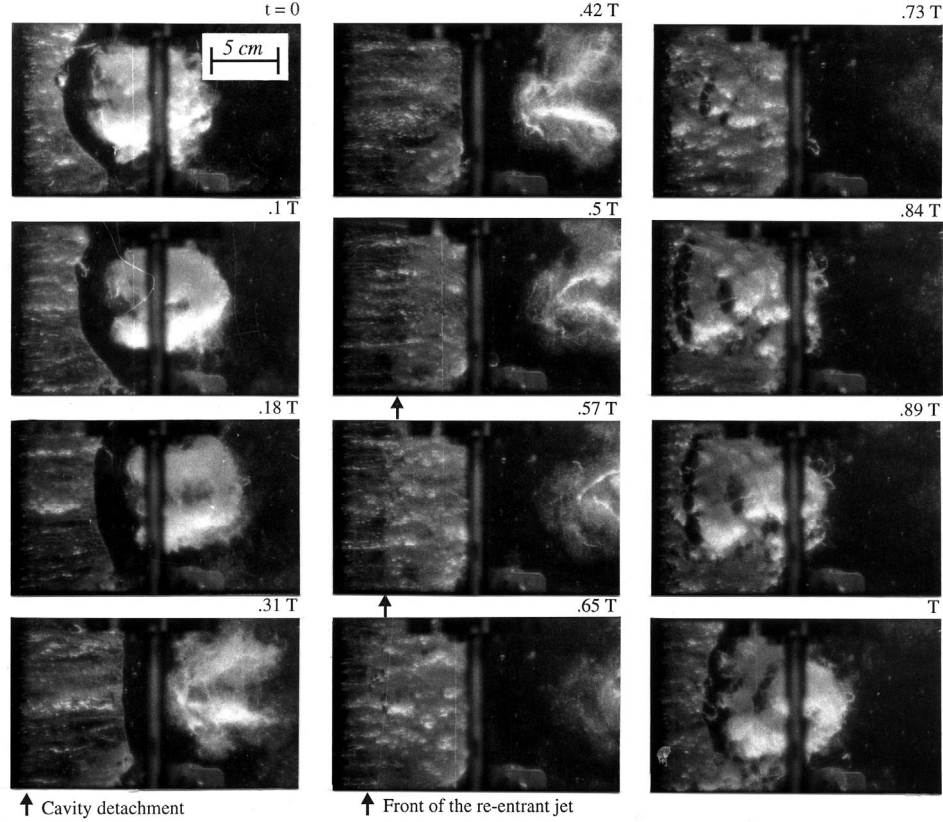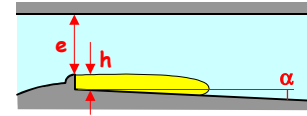
Figure 8: Visualization of the re-entrant jet and of the cavity oscillations (cloud cavitation) behind a diverging step. The flow velocity is 11.6 m/s. The geometry of the test section is shown here, the confinement height is e = 20 mm, the step height h = 3.6 mm, the divergence angle α = 4.2°. The period of the oscillation is 35 ms (Callenaere et al. 2001).

The decisive role of the re-entrant jet in the generation mechanism of cloud cavitation was experimentally proved by Kawanami *et al.* (1997). They conducted a simple but conclusive experiment which consisted in putting an obstacle on the foil in order to stop the progression of the re-entrant jet. As shown in Figure 9, the addition of such an obstacle holds back the re-entrant jet and prevents the generation of a large cloud. Much smaller vapour structures are formed. In addition, the pressure oscillations due to the shedding of the cloud are almost suppressed. This experiment definitely confirms the essential role of the re-entrant jet on the onset of cloud cavitation.

One of the pioneering works on the re-entrant jet instability is the study of Furness and Hutton (1975). The dynamic behaviour of the cavity which develops on a Venturi type nozzle is described and modelled by a two-dimensional unsteady potential flow theory. More recently, de Lange (1996) conducted a detailed computation of the dynamics of a cavity for two-dimensional hydrofoils, still using a boundary element method. Typical results are presented in Figure 10 and Figure 11. The roll-up motion at cavity closure which gives birth to the formation of the re-entrant jet is clearly visible. The re-entrant jet moves upstream and when it touches the upper cavity interface, the computation stops. In the case of Figure 10, the re-entrant jet reaches nearly the leading edge of the cavity. Although the computation is prematurely stopped because of the limitations of the BEM method, we can expect the shedding of a large vapour structure made of a large part of the attached cavity. It is the classical cloud cavitation phenomenon shown in Figure 8.
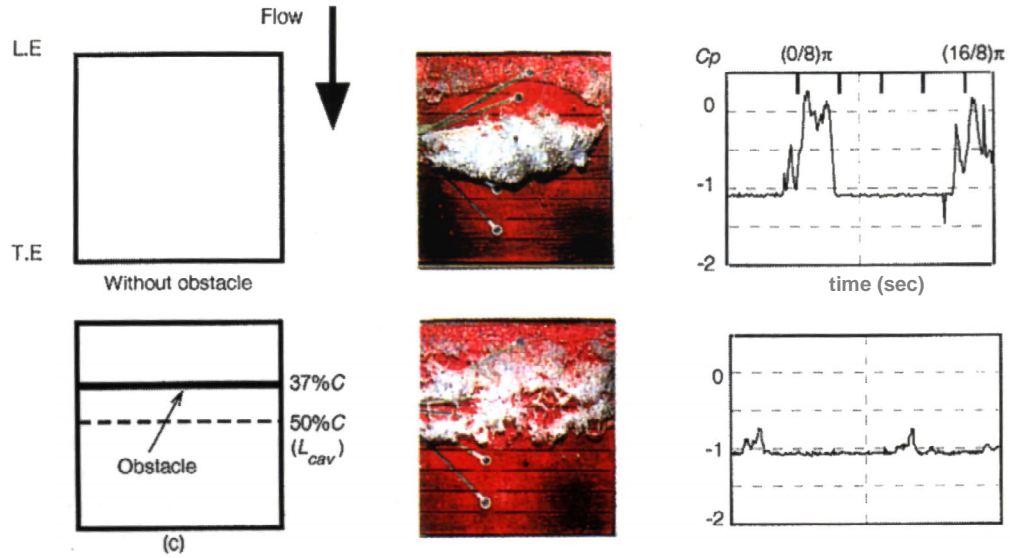
Figure 9: Mechanism and control of cloud cavitation (Kawanami et al. 1997). Two different cases are compared. The reference case of cloud cavitation on a smooth foil is presented on the top. The quasi inhibition of cloud cavitation by an obstacle is presented below.
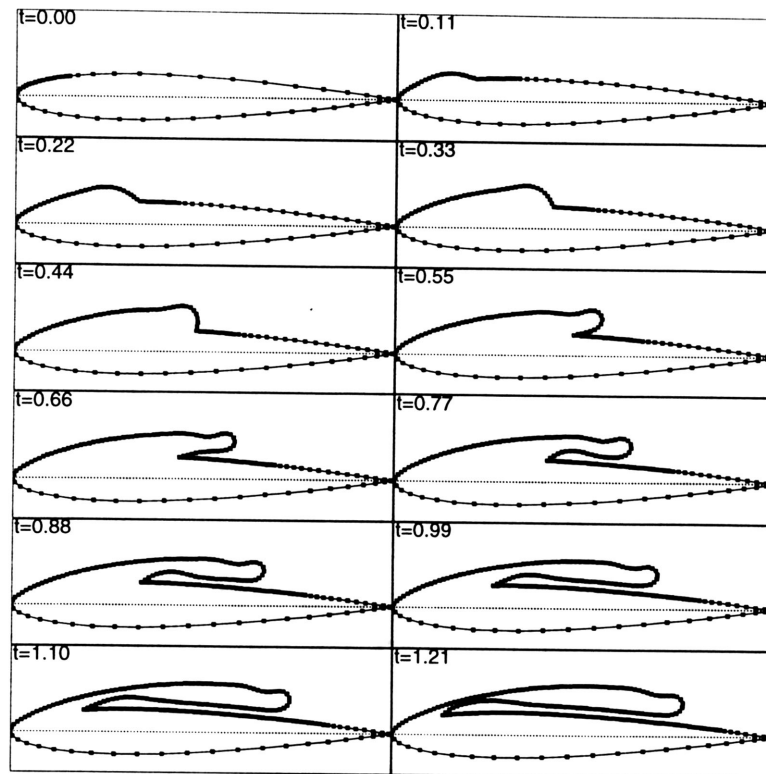

Figure 10 : Modeling of the cavity growth on a NACA 0012 profile at an angle of attack of 6°. and a cavitation number 0.25 (de Lange 1996)

In the second computational case presented in Figure 11, de Lange observes an early touching which does not necessarily prevents the re-entrant jet to continue its movement towards the leading edge of the cavity, as he conjectures. This phenomenon is probably the reason for the formation and shedding of small scale vapour structures which was observed experimentally by Callenaere *et al.* (2001). In their experiments, the cavity thickness is directly controlled by the height of the step which triggers the cavity. The higher the step height, the thicker the cavity. For a large step height and consequently a relatively thick cavity, they observe the classical cloud cavitation instability (see Figure 8). In the case of a relatively thin cavity, they still observe the development of a periodic re-entrant jet with a very comparable frequency. However, because of the smallness of the cavity thickness and consequently of the closeness of the cavity interface and the upper boundary of the re-entrant jet, a strong interaction exists between the cavity interface and the re-entrant jet, all along its upstream movement. The small scale instabilities which develop on both interfaces make that the thin vapour layer between the cavity interface and the re-entrant jet breaks at many points. Many small vapour structures are formed (see Figure 12), contrary to the unique large cloud shed by thicker cavities. In the case of cloud cavitation, the re-entrant jet does not interact significantly with the cavity interface as it moves upstream. The interaction is limited to the instant at which the re-entrant jet reaches the cavity leading edge and cuts the cavity interface. In conclusion, it appears that the characteristic size of the shedded structures depends upon the cavity thickness. Thick cavities shed large scale clouds, whereas much smaller scale structures are produced by thinner cavities.
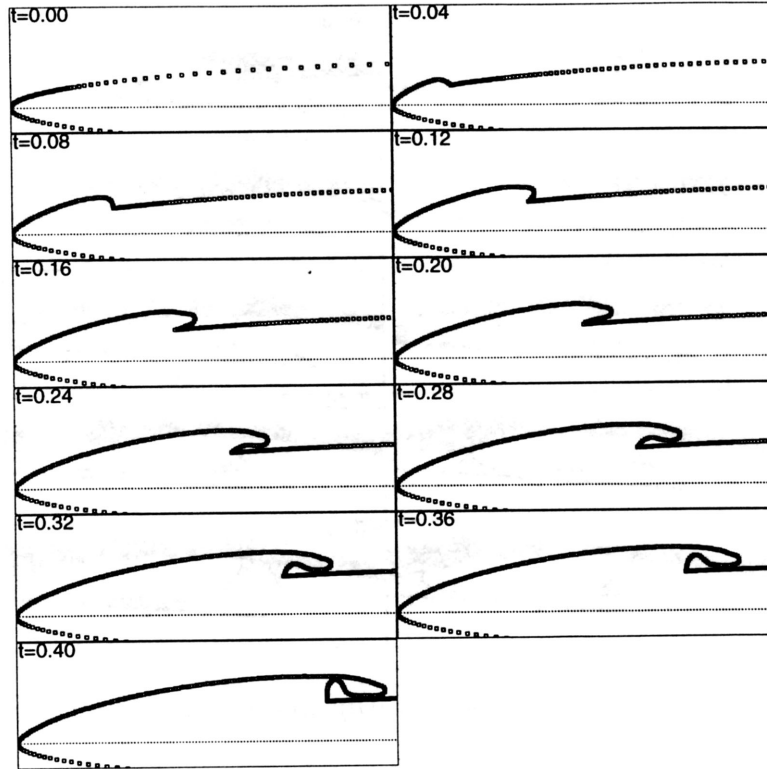

Figure 11: Modeling of the cavity growth on a NACA 16-009 profile at an angle of attack of 4° and a cavitation number 0.78 in the region x/c<0.4 (de Lange 1996)
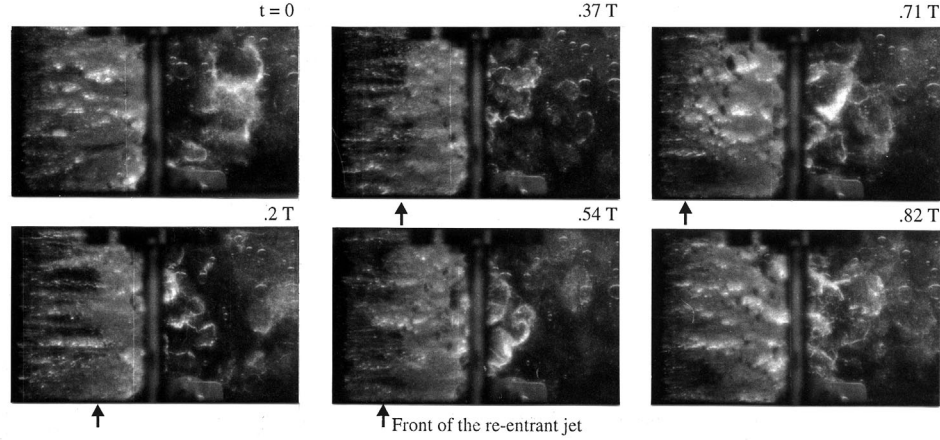
Figure 12: Visualization of the re-entrant jet and of the formation of small scale vapor structures in the case of a thin cavity. The geometry of the test section and the operating conditions are exactly the same as in Figure 8, except for the step height which is here equal to 0.8 mm instead of 3.6 mm. Hence, the only difference between Figure 8 and Figure 12 is the cavity thickness. The period of the oscillation is 36 ms. Although the front of the re-entrant jet is much more irregular than in the case of cloud cavitation, its location is indicated approximately by an arrow. (Callenaere et al. 2001).

Modelling aspects

From a modelling viewpoint, beside potential based panel methods mentioned above (see also Dang & Kuiper, 1998, 1999a, 1999b), an effort was made to develop models able to describe not only the growth phase of the sheet cavity and the development of the re-entrant jet, but also the break-off and the advection of the fully detached cloud that a Lagrangian description of the cavity contour fails to predict. Several approaches were used. Many of them model the liquid-vapour mixture as an homogeneous fluid of variable density. Different techniques have been developed to account for the variations in density.

In their local homogeneous model, Kubota (1988) and Kubota *et al.* (1992) assume that the flowing liquid carries cavitation nuclei. The nuclei density is an input parameter which has to be specified in the computation. Nuclei are convected and grow when they reach the low pressure region in the vicinity of the leading edge. Their growth is computed from a modified Rayleigh-Plesset equation, which takes into account the interaction between the bubbles. From the computation of the bubble cluster, it is possible to compute the void fraction and so the density of the mixture. This cavitation model is coupled with a Navier-Stokes solver to get the velocity and pressure fields. Figure 13 presents a typical visualization of cloud cavitation on a hydrofoil. The various mechanisms involved in this process including the growth of the leading edge cavity, the formation and the collapse of a cavitation cloud are correctly predicted. It has to be noticed that a simplified version of this model is now implemented in several commercial codes as Fluent and Star-CD.

Furthermore, separated two-phase flow models are being developed using a free surface tracking method as "volume of fluid" to capture the interfaces (see for example Dieval, 1999, Dieval *et al.*, 1998). For further information on the direct numerical simulation of free-surface flow and especially the VOF technique, the reader can refer to the review by Scardovelli & Zaleski (1999).

Barotropic models were also developed by several researchers (for example Reboud and Delannoy 1994, Song and He 1998, Shin & Ikohagi 1998, Arndt *et al.* 2000). The principle of the modelling still consists in considering an homogeneous liquid-vapour mixture. A state law of barotropic type is assumed for the mixture. It allows a continuous transition between the liquid density and the vapour density around the vapour pressure.
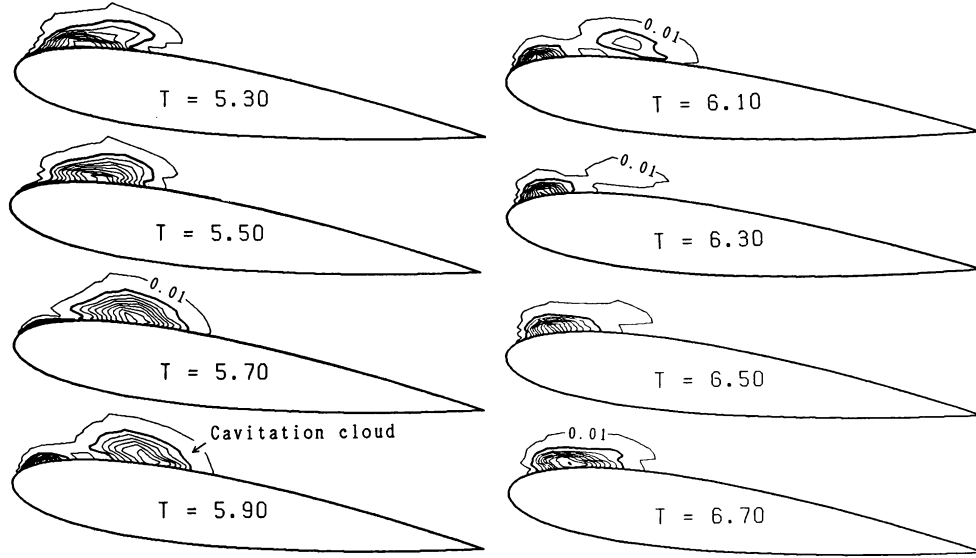
Figure 13: Void fraction contours around NACA0015 hydrofoil at an angle of attack of 8°, a Reynolds number of $3x10^5$ and a cavitation parameter of 1.0. The contour interval is 0.1 except for the most outer line. The nuclei density is 10^6 (reproduced from Kubota 1988).

Effect of the pressure gradient

It was already noticed that the mean pressure gradient has a significant influence on the re-entrant jet. Therefore, it is expected that the cloud cavitation instability will also depend upon the pressure gradient. This was proved by Callenaere *et al.* (2001) on a diverging step whose geometry is schematically shown in the caption of Figure 8. The domain of the cloud cavitation instability was determined visually and also from the measurement of the velocity fluctuations, as a function of the cavitation number and the height of the step (Figure 14). Let us recall that the step height directly controls the cavity thickness. The mean pressure gradient for the same configuration is shown in Figure 15. A comparison of both figures shows a good correlation between the domain of the cloud cavitation instability and the domain of high adverse pressure gradient.

This was confirmed by varying the adverse pressure gradient. This parameter was controlled by changing either the divergence angle α or the confinement height e of the channel (see caption of Figure 8 for the interpretation of α and e). A decrease in divergence angle as well as an increase in confinement height reduce the adverse pressure gradient and consequently significantly reduce the domain of the instability as presented in Figure 16. It was also observed that the cloud cavitation instability completely disappears in the case of a negligible adverse pressure gradient, corresponding to a larger confinement height e = 60 mm. In conclusion, the adverse pressure gradient has a crucial influence on the cloud cavitation instability and it can be conjectured that a critical adverse pressure gradient is necessary for the onset of this instability.

The previous results can help in the understanding of the onset of cloud cavitation in the case of a hydrofoil. Le *et al.* (1993a) have determined the domain of the cloud cavitation instability on a plano-convex hydrofoil. As shown in Figure 17, the cloud cavitation instability is observed for partial cavities whose length is around mid-chord. It does not occur for long cavities and in particular, no instability was observed between partial and supercavitation. Referring to the scheme in Figure 4, it can be inferred that the mean adverse pressure gradient decreases as the cavity length increases. Considering the necessity of a sufficiently high adverse pressure gradient for the onset of this instability, it is expected that cloud cavitation will occur for rather short cavities. Long cavities whose length is of the order of the chord length close in a region where the pressure distribution is relatively flat. Therefore, long cavities should not exhibit the cloud cavitation instability. If oscillations in cavity length actually occur, as observed for instance by Wade & Acosta (1966), they are most likely of surge type and related to the extreme sensitivity of long cavities to external pressure fluctuations already discussed.
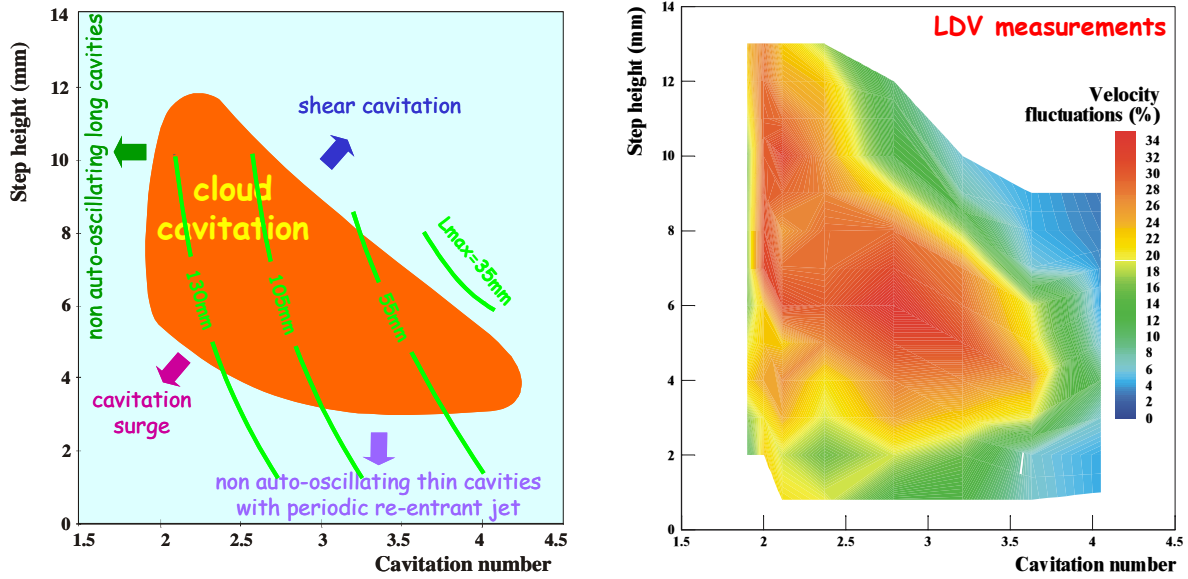
11

Figure 14: The domain of cloud cavitation on a diverging step as a function of the cavitation number and the height of the step. The diagram on the left corresponds to a visual determination of the domain of instability under stroboscopic lighting, whereas the diagram on the right was obtained from velocity fluctuation measurements. The geometry of the test section is schematically given in the caption of Figure 8. The flow velocity is 11.6 m/s, the confinement height is e = 20 mm and the divergence angle is α = 4.2° (Callenaere et al. 2001)
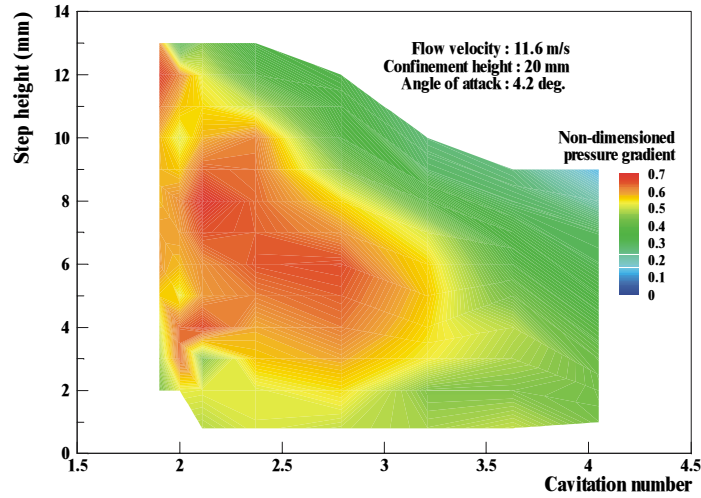

Figure 15: Mean adverse pressure gradient corresponding to the configuration presented in Figure 14. The pressure gradient was estimated from LDV measurements (Callenaere et al. 2001).
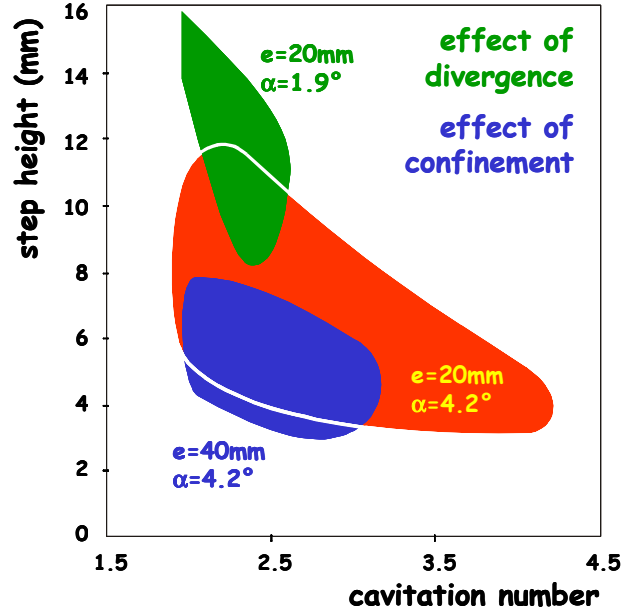
Figure 16: Influence of the adverse pressure gradient on the domain of cloud cavitation instability observed on a diverging step. The pressure gradient is controlled either by the divergence or the confinement of the channel. The domain of cloud cavitation instability is significantly reduced when the adverse pressure gradient is reduced (Callenaere et al. 2001).
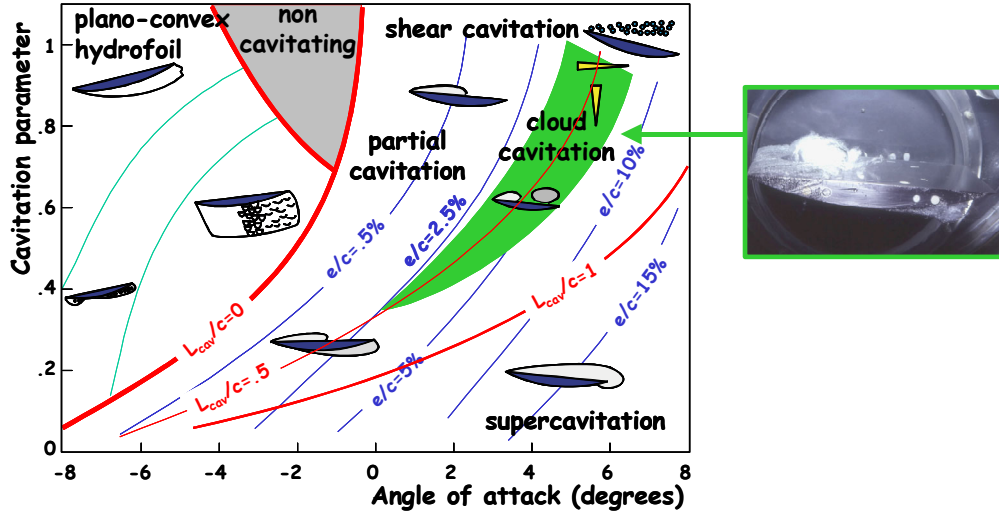

Figure 17: Various cavitation patterns observed on a plano-convex hydrofoil as a function of the angle of attack and of the cavitation parameter. The region in green corresponds to the domain of cloud cavitation instability characterized by the periodic shedding of vapor clouds. The cavity length L_{cav} and the cavity thickness e, non dimensioned by the chord length c, are indicated (Le et al. 1993a).

As a consequence, it appears difficult to control the instability of partial cavitation on a hydrofoil. A strong adverse pressure gradient is favourable to the re-entrant jet instability, whereas a negligible pressure gradient will make the cavity more sensitive to external fluctuations and hence more sensitive to cavitation surge. Thus, we can swing from an intrinsic instability to a system instability with an increase in cavity length. Both instabilities can even coexist, as proved by pressure spectra (see Figure 22).

From Figure 17, it appears that very short cavities on a hydrofoil do not exhibit the cloud cavitation instability. Although they close in a region of high adverse pressure gradient, their thickness is so small that the re-entrant jet

does not lead to the formation of a unique large cloud but of many small vapour structures all along its upward movement. This difference was already illustrated in Figure 8 and Figure 12.

In conclusion, the onset of the cloud cavitation instability requires two main conditions:

1. The cavity must close in a region of large enough adverse pressure gradient favourable to the development of the re-entrant jet
2. The cavity must be thick enough to limit the interaction between the re-entrant jet and the cavity interface during its movement to the leading edge, allowing thus the formation of a unique large vapour structure

Advanced measurements

In 1989, Kubota *et al.* gave a detailed description of the flow structure around unsteady cloud cavitation on a stationary two-dimensional hydrofoil by laser Doppler anemometry using a conditional sampling technique. They showed that the shedded cloud is a large-scale vortex structure containing many small cavitation bubbles. Yamaguchi *et al.* (1990) succeeded to measure the micro-scale structure of the cavitation cloud using a laser holography system. They were able to quantify the bubble distribution as a function of their diameter. The pressure pulses induced by the collapse of those bubbles were measured by Le *et al.* (1993b). Their pressure pulse height spectra confirm the well-known industrial observation according to which, from an erosion viewpoint, cloud cavitation is much more aggressive than a stable sheet cavity. To reduce the aggressiveness, several possibilities were tested by Boehm *et al.* (1997, 1998) including variations of the leading edge geometry, air injection and the insertion of an obstacle to stop the re-entrant jet.

The structure of the two-phase flow inside the cavity was investigated by Stutz and Reboud (1997) and Reboud *et al.* (1998) using a double optical probe. They succeeded to measure the local void fraction and the velocity inside their cavities and showed that, for their cavitating conditions, the void fraction does not exceed 21%. Their velocity measurements also confirm the existence of a reversed two-phase flow along the wall. Other experimental techniques were used to investigate the structure of partial attached cavities as laser Doppler anemometry (Avellan and Dupont, 1988, Dupont, 1993), particle imaging velocimetry (Laberteaux and Ceccio, 1998, 2001a, 2001b) and electrical impedance probes (George *et al.*, 2000, Pham *et al.*, 1998).

The re-entrant jet thickness was measured by Callenaere *et al.* (2001) by an ultrasonic technique on the diverging step already presented. Typical results are given in Figure 18. The cavity thickness and the re-entrant jet thickness are plotted as a function of the step height. The cavity thickness increases like the step height, whereas the re-entrant jet thickness increases not as much. Thus, the thickness of the vapour layer between the re-entrant jet and the cavity interface changes considerably with the cavity thickness. For thick enough cavities, this vapour layer is so thick that no significant interaction exists between the re-entrant jet and the cavity interface. On the contrary, when the cavity thickness decreases, the interaction becomes more and more significant. Below a threshold value of the cavity thickness, the surface perturbations which travel on both interfaces make that the thin vapour layer breaks in a large number of small scale vapour structures. This discussion confirms that the cloud cavitation instability can develop only if the thickness of the cavity is large enough, in comparison with the re-entrant jet thickness.

Returning to the influence of the pressure gradient on the re-entrant jet thickness, a quick estimate of the re-entrant jet thickness can be made on the basis of Equation 7 and compared with the previous experimental results. Without any pressure gradient, the re-entrant jet thickness λ_0, non-dimensioned by the cavity thickness, can be estimated around a few percents only (see Figure 6 and also Laberteaux & Ceccio 2001a). This thickness is increased by the adverse pressure gradient according to Equation 7. Referring to Figure 16, the non-dimensioned pressure gradient $dC_p / d(x / L)$ where L is the maximum cavity length, is of the order of 0.6 in the domain of cloud cavitation. Therefore, the increase in the non-dimensioned re-entrant jet thickness due to the adverse pressure gradient is around 15%, which is much greater than the few original percents. Hence, the re-entrant jet thickness is mostly controlled by the adverse pressure gradient. These estimates are roughly in agreement with the experimental results which give a range of variation of the non-dimensioned re-entrant jet thickness between 15% and 30% according to the operating conditions (Callenaere *et al.*, 2001).
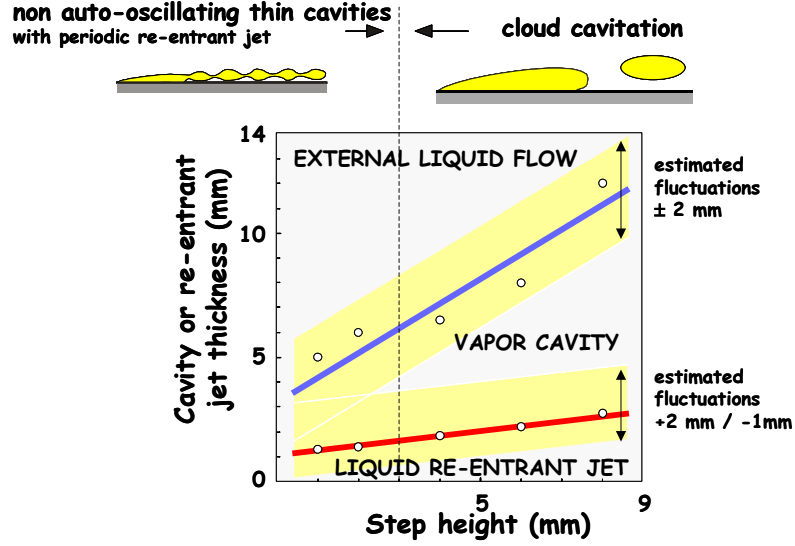
Figure 18: Evolution of the thickness of the re-entrant jet and of the cavity as a function of the step height, in the case of a diverging step. The flow velocity is 11.6 m/s, the confinement height is e = 20 mm, the divergence angle is α = 4.2° and the maximum cavity length is about 95 mm (Callenaere et al., 2001).

As for the re-entrant jet velocity, most studies conclude that it is of the order of the main flow velocity (see e.g. Pham et al, 1998). Variations can be expected according to the thickness of the cavity. For example, Callenaere *et al.* (2001) have shown that, in the case mentioned above of thin cavities for which a strong interaction exists between the re-entrant jet and the cavity interface, the re-entrant jet is "braked" by the cavity interface. A few measurements tend to prove that its mean velocity is only about 60% of its velocity in the reference case of cloud cavitation for which the interaction of the re-entrant jet with the cavity interface can be considered as negligible. In a similar way, we can expect a decelerating effect of the wall roughness on the re-entrant jet.

Three-dimensional aspects

In the fully two-dimensional case, the re-entrant jet velocity is parallel to the main flow velocity, and directed in the opposite direction. As explained by de Lange (1996), the re-entrant jet velocity gains a spanwise component if the closure line of the cavity is inclined. Assuming that the pressure gradient has no component along the closure line, the conservation of the tangential momentum implies that the velocity component tangential to the closure line remains unchanged. It results that the incident velocity is reflected at the closure line as schematically shown in Figure 19.
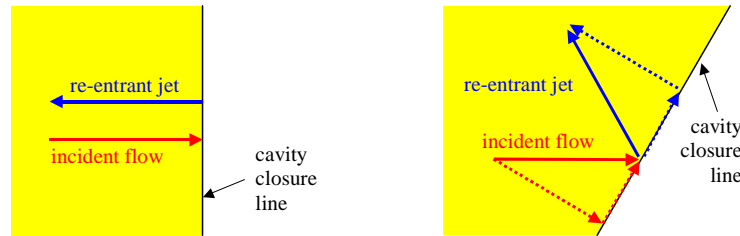

Figure 19: Reflection of the incident flow by the closure line of the cavity. The flow is from left to right. (adapted from de Lange, 1996).

This phenomenon happens in the case of a swept foil, as illustrated by the photograph of Figure 20 taken by Laberteaux and Ceccio (2001). Two very different regions in the cavity interface are clearly visible. Part of the cavity is glossy and rather steady, whereas the rest of the interface is frothy and more unsteady. The interpretation of this photograph is given in Figure 21 reproduced from Duttweiler & Brennen (1998). The re-entrant jet flow can be divided into two parts. In the upstream region where the closure line is very inclined, the re-entrant jet never reaches

the leading edge and thus delimits a vapour-filled cavity, whereas in the downstream part where the closure line is less inclined, the re-entrant jet, by impinging on the cavity interface, generates a liquid-vapour mixture.

Even in the case of purely two-dimensional experiments, it is often observed that the closure line of the sheet cavity has a convex shape (see for instance Figure 1). Thus, three-dimensional effects can be suspected as mentioned by de Lange (1996).
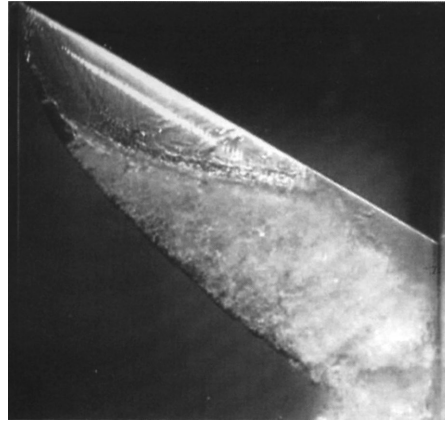

Figure 20: Cavitation on a three-dimensional hydrofoil with 30° of sweep, at 2° of angle of attack,
for a flow velocity of 10.1 m/s and a cavitation parameter of 0.7. The flow is downward.
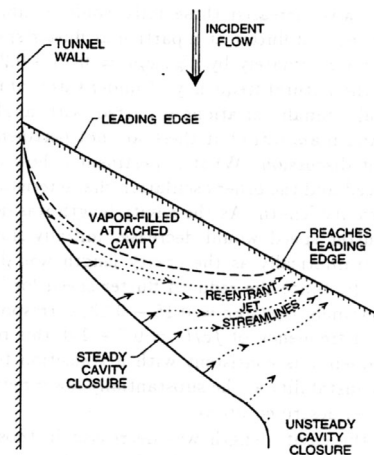*Reproduced from Laberteaux and Ceccio (2001b)*

Figure 21: Interpretation of the photograph of Figure 20. Reproduced from Duttweiler and Brennen (1998).

Frequency content

From visualizations under stroboscopic lighting, it is possible to measure the characteristic frequency of the cloud cavitation instability. This technique is easy to handle when the shedding is regular, but is more and more unreliable as the limits of the periodic domain are approached. The use of pressure transducers and the spectral analysis of pressure fluctuations offers a more objective approach. Arndt *et al.* (2000) and Kjeldsen *et al.* (1998) make use of a joint time-frequency analysis on ramping tests to identify the frequency content of partial cavity instabilities.

In their analysis of partial cavitation on a diverging step, Callenaere *et al.* (2001) made a spectral analysis of the pressure fluctuations measured by a pressure transducer located at the observed cavity closure, for different cavity lengths. For each cavity length, several step heights were considered and a spectrum was obtained for each of them. All the spectra corresponding to the various step heights are juxtaposed to get the maps shown on Figure 22. For the short cavity considered here (75 mm), the cloud shedding frequency is easily identified. It corresponds to a Strouhal

number close to 0.2. The lower and upper limiting values of the step height for which the peak in the spectra vanishes are in agreement with the mapping of the cloud cavitation instability presented on Figure 14. For the long cavity (150 mm), another maximum is visible on the spectra at a lower frequency. This second frequency is the signature of a second instability which is likely of surge type because it affects only long cavities that close in regions of small adverse pressure gradient. Figure 22 shows that both instabilities can occur simultaneously. As the cavity length is increased, the kind of instability which affects partial cavitation progressively changes from the cloud cavitation instability to a cavitation surge instability.
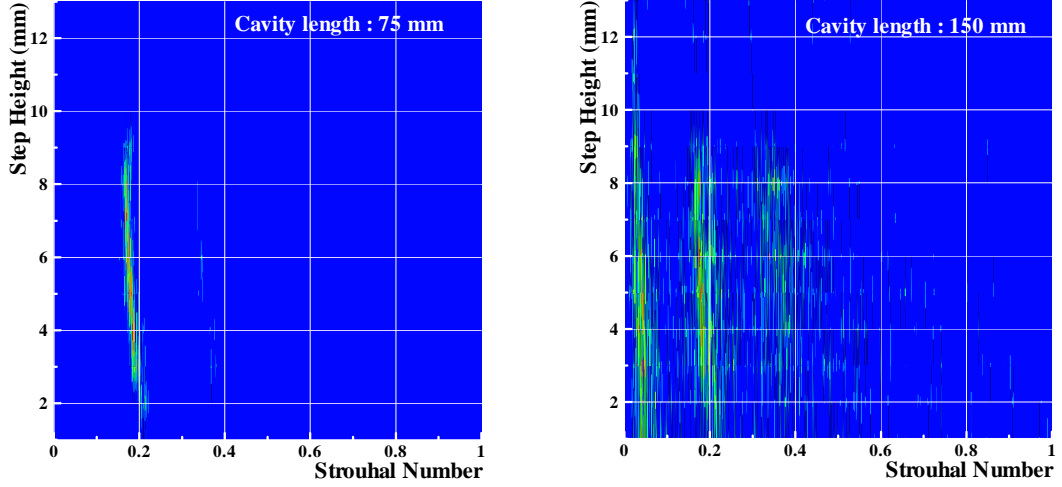

Figure 22: Spectra of the pressure fluctuations at cavity closure. Each diagram corresponds to a given cavity length. The spectra obtained for various steps heights are piled up. The tested geometry is the diverging step represented in the caption of Figure 8. The flow velocity is 11.6 m/s, the confinement height is e = 20 mm and the angle of divergence α is 4.2° (Callenaere et al., 2001).

Finally, let us mention that the higher frequency content of the pressure fluctuations was analysed by Reisman, Wang and Brennen (1998). They distinguish global and local events. The global events are essentially the coherent collapse of large scale clouds which generates an overpressure simultaneously detected by all the transducers located in the collapsing zone. On the contrary, local events are randomly distributed and correspond to the collapse of small scale vapour structures. They are interpreted as shock waves in the bubbly mixture by Reisman *et al.*

3.   Other intrinsic instabilities

The cloud cavitation instability, triggered by the re-entrant jet, is the most well-known instability of intrinsic type that a partial cavity can experience. However, other intrinsic instabilities have either been observed experimentally or predicted from computation. We would like to mention here the three-dimensional shedding observed by Kawanami *et al.* (1998) on two-dimensional hydrofoils and the high-frequency instabilities that a linear analysis of partial cavitation reveals (Watanabe *et al.* 1998).

Three-dimensional shedding

In the previous section, we focused on the typical cloud cavitation instability which sheds a unique large vapour structure. Kawanami *et al.* (1998) have shown that, still on two-dimensional hydrofoils, other regimes of shedding can take place and that a certain spatial periodicity exists along the spanwise direction. The photographs in Figure 23 present the case of partial cavities which shed simultaneously several clouds along the span. Kawanami *et al.* measured the spanwise length of the clouds which are shed by a partial cavity. They showed that it is correlated to the usual cavity length. Roughly speaking, the spanwise length of the clouds is of the order of the cavity length and hence, the number of clouds simultaneously shed along the span increases as the cavity length is reduced. Although such results may be dependent upon the facility as we can imagine a particular matching of the three-dimensional shedding to the width of the test section, they prove that other instabilities of three-dimensional type can affect partial cavities.
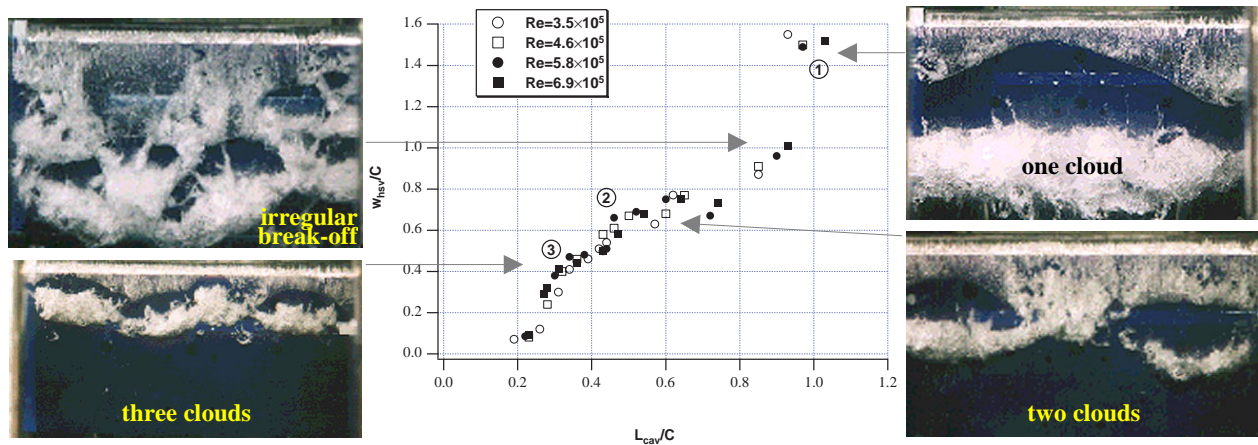

Figure 23: Variation of the spanwise length of cloud cavities with the chordwise length of the partial sheet cavity. Both lengths are non-dimensioned by the chord length (from Kawanami et al. 1998)

High-frequency instabilities

Finally, we mention the possible occurrence of high-frequency instabilities which can be expected from a linear analysis of the stability of two-dimensional closed partial cavities. Watanabe *et al.* (1998) have computed various modes of instability, presented in Figure 24. Mode I, which occurs at zero frequency, is the instability already mentioned between partial and supercavitation. It is due to a negative cavitation compliance. Mode II and mode III are high frequency modes. As shown by the temporal evolution of the cavity, they correspond to periodic oscillations of the interface. Mode I corresponds to a downstream travelling wave on the cavity interface, with one wavelength, whereas mode II corresponds to a two wavelengths regime. Although such instabilities were not yet observed experimentally, we must keep in mind that the linear stability theory predicts the possibility of development of high-frequency instabilities.
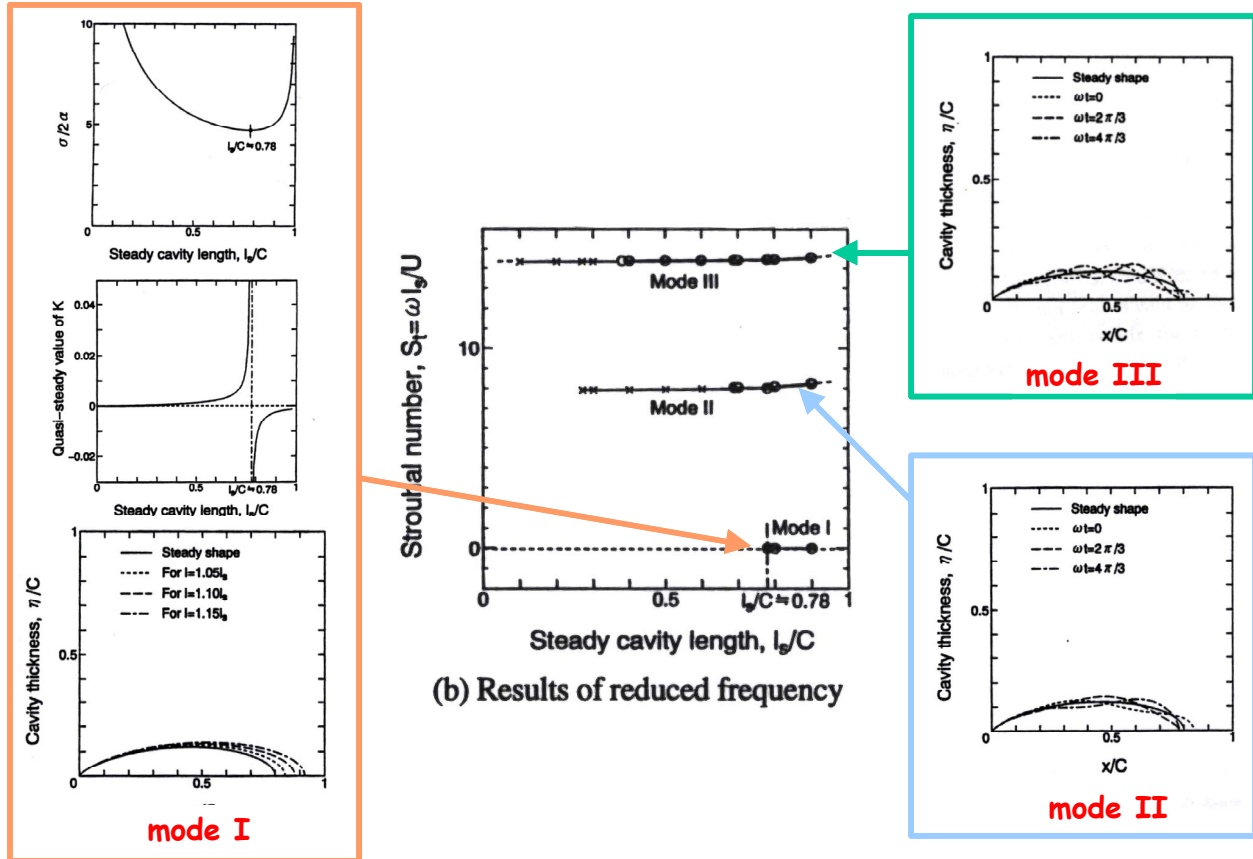
Figure 24: Various modes of instability deduced from a linear analysis of the stability of two-dimensional partial cavities. The central part of the figure gives the Strouhal number of modes I, II and III. The evolution in time of the cavity interface is also indicated for each mode (reproduced from Watanabe et al. 1998).

4. Concluding remarks

Partial cavities may experience various forms of instabilities which can be either system dependent or purely intrinsic. The determination of the cause of an instability is often made difficult by the coupling of the cavitation with the environment or the facility. The comparison of tests conducted on various geometries, for various operating conditions and in different facilities has recently allowed a better physical understanding of partial cavitation instabilities. From a modelling viewpoint, several models have been developed to compute the unsteady behaviour of partial cavities. Very encouraging results, showing qualitative (and more rarely quantitative) agreement with experiments, have been obtained from the use of cavitation models, coupled with Navier-Stokes solvers. Each model has its own specificities and also its own numerical or physical adjusted parameters. Hence, an effort has to be made to carry out a large enough number of comparative computations on various test cases (which is not so easy in practice as such models are generally very time consuming) in order to identify their limitations and provide the cavitation community with validated predicting tools.

References

Arndt R., Song C., Kjeldsen M., He J. & Keller A. 2000 "Instability of partial cavitation: a numerical/experimental approach" *Proc. 23rd Symp. On Naval Hydrodynamics* Val de Reuil France Sept.17-22 140-155

Avellan F. & Dupont P. 1988 "Etude du sillage d'une poche de cavitation partielle se développant sur un profil hydraulique bi-dimensionnel" *La Houille Blanche* **7/8** 507-515

Belahadji B., Franc J.P. & Michel J.M. 1997 "Analyse des effets thermiques en cavitation à partir d'essais au forane"

La Houille Blanche **4/5** 117-122

Boehm R., Stoffel B. & Ludwig G. 1997 "Investigations on the unsteady behaviour of cavitation and the corresponding pressure field" *La Houille Blanche* **4/5** 84-88

Boehm R., Hofmann M., Ludwig G. & Stoffel B. 1998 "Investigations on possibilities to control the erosive cavitation aggressiveness by hydrodynamic effects" *Proc. of the Third Int. Symp. on Cavitation* **Vol.2** 121-127 ed. J.M. Michel and H. Kato

Brennen C.E. 1995 "Cavitation and bubble dynamics" *Oxford Univ. Press*

Callenaere M., Franc J.P., Michel J.M. & Riondet M. 2001 "The cavitation instability induced by the development of a re-entrant jet" submitted for publication in the Journal of Fluid Mechanics

Ceccio S.L. & George D.L. 1996 "A review of electrical impedance techniques for the measurement of multiphase flows" *J. of Fluids Eng.* **118** 391-399

Dang J. & Kuiper G. 1998 "Re-entrant jet modelling of partial cavity flow on two-dimensional hydrofoils"*Proc. of the Third Int. Symp. on Cavitation* **Vol.2** 233-242 ed. J.M. Michel and H. Kato

Dang J. & Kuiper G. 1999a "Re-entrant jet modelling of partial cavity flow on two-dimensional hydrofoils"*J. of Fluids Eng.* **Vol.121** December 1999 773-780

Dang J. & Kuiper G. 1999b "Re-entrant jet modelling of partial cavity flow on three-dimensional hydrofoils"*J. of Fluids Eng.* **Vol.121** December 1999 781-787

De Lange D.F., de Bruin G.J. & van Wijngaarden L. 1994 "On the mechanism of cloud cavitation - Experiment and modelling" *Proc. of the Second Int. Symp. on Cavitation* 45-49 ed. H.Kato

De Lange D.F. 1996 "Observation and modelling of cloud formation behind a sheet cavity" *PhD thesis* Univ. of Twente, The Netherlands

Dieval L. 1999 "Simulation des écoulements cavitants par poche par une méthode de suivi d'interface" *PhD thesis* Univ. of Aix-Marseille II, France

Dieval L., Arnaud A. & Marcer R. 1998 "Numerical modeling of unsteady cavitating flows by a VOF method" *Proc. of the Third Int. Symp. on Cavitation* **Vol.2** 243-248 ed. J.M. Michel and H.Kato

Dupont P. 1993 "Etude de la dynamique d'une poche de cavitation partielle en vue de la prédiction de l'érosion dans les turbomachines hydrauliques" *PhD thesis* Ecole Polytechnique Fédérale de Lausanne, Switzerland

Duttweiler M.E. 2001 "Surge instability on a cavitating propeller" *Thesis* California Institute of Technology Pasadena California

Duttweiler M.E. & Brennen C.E. 1998 "Partial cavity instabilities" *Proc. of US-Japan seminar: Abnormal Flow Phenomena in Turbomachines* Nov. 1-6 Osaka Japan

Furness R.A. & Hutton S.P. 1975 "Experimental and theoretical studies of two-dimensional fixed-type cavities" *J. of Fluids Eng.* **97** 515-522

George D.L., Iyer C.O. & Ceccio S.L. 2000 "Measurement of the bubbly flow beneath partial attached cavities using electrical impedance probes" *J. of Fluids Eng.* 122 151-155

Kawanami Y., Kato H., Yamaguchi H., Tagaya Y. & Tanimura M. 1997 "Mechanism and control of cloud cavitation" *J. of Fluids Eng.* **119** 788-795

Kawanami Y., Kato H. & Yamaguchi H. 1998 "Three-dimensional characteristics of the cavities formed on a two-dimensional hydrofoil" *Proc. of the Third Int. Symp. on Cavitation* **Vol.1** 191-196 ed. J.M. Michel and H. Kato

Kjeldsen M., Effertz M. & Arndt R.E.A. 1998 "Investigation of unsteady cavitation phenomena" Proc. Of US-Japan Seminar Abnormal Flow Phenomena in Turbomachines Nov.1-6 Osaka Japan

Kubota A. (1988) "Numerical studies of unsteady cavitation on a hydrofoil by a bubble two-phase flow model" *PhD thesis* University of Tokyo, Japan

Kubota A., Kato H., Yamaguchi H. & Maeda M. 1989 "Unsteady structure measurement of cloud cavitation on a foil section using conditional sampling technique *J. of Fluids Eng.* **111** 204-210

Kubota A., Kato H. & Yamaguchi H. 1992 "A new modelling of cavitating flows: a numerical study of unsteady cavitation on a hydrofoil section" *J. Fluid Mech.* **240** 59-96

Laberteaux K.R. & Ceccio S.L. 1998 "Flow in the closure region of closed partial attached cavitation" *Proc. of the Second Int. Symp. on Cavitation* **Vol.1** 197-202 ed. J.M. Michel and H. Kato

Laberteaux K.R. & Ceccio S.L. 1998 "Partial attached cavitation on two- and three-dimensional hydrofoils" *Proc. 22nd ONR Symp. on Naval Hydrodynamics*, Washington DC

Laberteaux K.R. & Ceccio S.L. 2001a "Partial cavity flows. Part 1. Cavities forming on models without spanwise variation" *J. Fluid Mech* **431** 1-41

Laberteaux K.R. & Ceccio S.L. 2001a "Partial cavity flows. Part 2. Cavities forming on test objects with spanwise variation" *J. Fluid Mech* **431** 43-63

Le Q., Franc J.P. & Michel J.M. 1993a "Partial cavities : global behaviour and mean pressure distribution" *J. of Fluids Eng.* **115** 243-248

Le Q., Franc J.P. & Michel J.M. 1993b "Partial cavities : pressure pulse distribution around cavity closure" *J. of Fluids Eng.* **115** 249-254

Lemonnier H. & Rowe A. 1988 "Another approach in modeling cavitating flows" *J. Fluid Mech.* **195** 557-580

Michel J.M. 1978 "Demi-cavité formée entre une paroi solide et un jet plan de liquide quasi parallèles: approche théorique" *DRME 77/352 N°4 report*

Pham T.M., Larrarte F. & Fruman D.H. 1998 "Investigation of unstable cloud cavitation" *Proc. of the Third Int. Symp. on Cavitation* **Vol.1** 215-220 ed. J.M. Michel and H. Kato

Reisman G.E., Wang Y.-C. & Brennen C.E. 1998 "Observations of shock waves in cloud cavitation" *J. Fluid Mech.* **355** 255-283

Reboud J.L. & Delannoy Y. 1994 "Two-phase flow modelling of unsteady cavitation" *Proc. of the Second Int. Symp. on Cavitation* 39-44 ed. H. Kato

Reboud J.L., Stutz B. & Coutier O. 1998 "Two-phase flow structure of cavitation : experiment and modelling of unsteady effects" *Proc. of the Second Int. Symp. on Cavitation* **Vol.1** 203-208 ed. J.M. Michel and H. Kato

Scardovelli R. & Zaleski S. 1999 "Direct numerical simulation of free-surface and interfacial flow" Annu. Rev. Fluid Mech. **31** 567-603

Shin B.R. & Ikohagi T. 1998 "A numerical study of unsteady cavitating flows" *Proc. of the Second Int. Symp. on Cavitation* **Vol.2** 301-306 ed. J.M. Michel and H. Kato

Song C.C.S. & He J. 1998 "Numerical simulation of cavitating flows by single-phase flow approach" *Proc. of the Third Int. Symp. on Cavitation* **Vol.2** 295-300 ed. J.M. Michel and H. Kato

Stutz B. & Reboud J.L. 1997 "Experiments on unsteady cavitation" *Experiments in Fluids* **22** 191-198

Tsujimoto Y. 1995 "Rotating cavitation: knowns and unknowns", *Proc. of the 1995 ASME/JSME Fluids Eng. Div. Summer Meeting*

Tsujimoto Y. 2001 "Simple rules for cavitation instabilities in turbomachinery" *Proc. 4th Int. Symp. on Cavitation* June 20-23 Pasadena California USA

Wade R.B. & Acosta A.J. 1966 "Experimental observations on the flow past a plano-convex hydrofoil" J. *of Basic Eng.* **87** 273-283

Watanabe S., Tsujimoto Y., Franc J.P. & Michel J.M. 1998 "Linear analyses of cavitation instabilities", *Proc. of the Third Int. Symp. on Cavitation* **Vol.1** 347-352 ed. J.M. Michel and H. Kato

Watanabe S., Sato K., Tsujimoto Y., Kamijo K. 1999 "Analysis of rotating cavitation in a finite pitch cascade using a closed cavity model and a singularity method", *J. of Fluids Eng.* **Vol.121** December 1999 834-840

Yamaguchi H. & Kato H. 1993 "On application of nonlinear cavity flow theory to thick foil sections" *2nd Int. Conf. On Cavitation* Edinburgh 6-8 Sept.1983 **C209/83** 167-174

Yamaguchi H., Kato H., Kamijo A. & Maeda M. 1990 "Development of a laser holography system for the measurement of cavitation bubble clusters", *ASME 1990 Cavitation and Multiphase Flow Forum*